IOP Conf. Series: Materials Science and Engineering **274** (2017) 012062 doi:10.1088/1757-899X/274/1/012062

Application and Analysis of Measurement Model for Calibrating Spatial Shear Surface in Triaxial Test

Zhihua Zhang *, Hongsheng Qiu, Xiedong Zhang and Hang Zhang

School of Transportation, Wuhan University of Technology, Wuhan 430063, China

*Corresponding author e-mail: zzh@whut.edu.cn

Abstract. Discrete element method has great advantages in simulating the contacts, fractures, large displacement and deformation between particles. In order to analyze the spatial distribution of the shear surface in the three-dimensional triaxial test, a measurement model is inserted in the numerical triaxial model which is generated by weighted average assembling method. Due to the non-visibility of internal shear surface in laboratory, it is largely insufficient to judge the trend of internal shear surface only based on the superficial cracks of sheared sample, therefore, the measurement model is introduced. The trend of the internal shear zone is analyzed according to the variations of porosity, coordination number and volumetric strain in each layer. It shows that as a case study on confining stress of 0.8 MPa, the spatial shear surface is calibrated with the results of the rotated particle distribution and the theoretical value with the specific characteristics of the increase of porosity, the decrease of coordination number, and the increase of volumetric strain, which represents the measurement model used in three-dimensional model is applicable.

1. Introduction

Coarse grained soil as a crucial engineering material has been widely used in geotechnical constructive engineering in recent decades. The variation of the content of stones and moisture leads to the complicated characteristics of coarse grained soil. In landslide cases, soil losses its stability with different failure model and the distribution of the spatial failure surface is difficult to be evaluated. Therefore, the failure evolution has been the main content for studying the strength and deformation characteristics of coarse grained soil.

Discrete element method (DEM), has its great advantages in simulating the mechanism, stability, deformation and constitutive relation of particle material, was proposed by Cundall[1]. In micro crack simulations, Stefan[2] discussed the evolution of cracks of granular materials during the compression; Muhlhaus and Vardoulakis[3] studied the thickness of shear band based on DEM that the formation of shear band was due to the furcation charactertistic of granular soil; Oda[4] and Zhang[5] evaluated the formation of shear surface and the mechanism of shear dilation that the evolution of cracks in the cohesive material was associated with shear dilation; Jiang[6-7] concluded that the thickness of the shear band was 10-15 times larger than the diameter of dense sand with obvious particle rotation; Vardoulakis[8] analyzed the initial defection of sand based on the plane strain experiences that the deformation occurred first in the defection area and had relationship with the area size which was consistent with the conclusion made by Zhou[9]. In general, the measurement model inserted in

numerical sample can history the crack formation and the evolution of the shear surface, however, little has been published on this subject.

In this paper, triaxial test model is conducted based on DEM. The numerical results is first consistent with that in laboratory. The sample used in the model is proposed by the weighted average assembling method [10]. Measurement model is inserted in the sample with 133 measurement spheres to history the variations of coordination number, porosity and volumetric strain during shearing. Spatial shear surface is calibrated with characteristics of the measured data, the rotated particle field and the theoretical result.

2. Triaxial Test

The triaxial test was conducted by using the computer servo-controlled triaxial test appratus[11]. The coarse grained soil was taken from the dam of Shuibuya. Some selected parameters, such as maximum dry density ρ_{dmax}, minimum dry density ρ_{dmin}, liquid limit w_L, plastic limit w_p and plasticity index I_p had been measured based on Specification of Soil Test (SL 237-1999), which are shown in Table 1.

Table 1. Basic parameters of the coarse grained soil in triaxial test.

Parameter	ρ_{dmax}	ρ_{dmin}	w_L	w_p	I_p
Unit	kg/m^3	kg/m^3	%	%	%
Value	2340	1800	28.34	17.62	10.72

Triaxial tests were conducted under confining stresses of 0.8, 1.6 and 3.3 MPa with the sample size of 300×600 mm (Diameter ×Height), as shown in Fig. Bulk density of the initial sample was 2180 kg/m^3.

3. Model Setup and Measurement Model

3.1. Numerical Model of Triaxial Test

Granular materials are generated in a cylindrical wall with two planes on the top and bottom. The sample is assembled by the weighted average method[10] for good consistence with that of laboratory in particle size distribution. The cylindrical wall keeps the confining stress with the servo-control system, while the top plane loads the sample with the fixed bottom plane. The curves of particle size distribution of the sample in numerical model and experimental test are shown in Fig. 1 that great consistence lead to the suitable simulation in triaxial test. Referring to the literature of Zhang et al. [10], the numerical model of triaxial test is shown in Fig. 2.

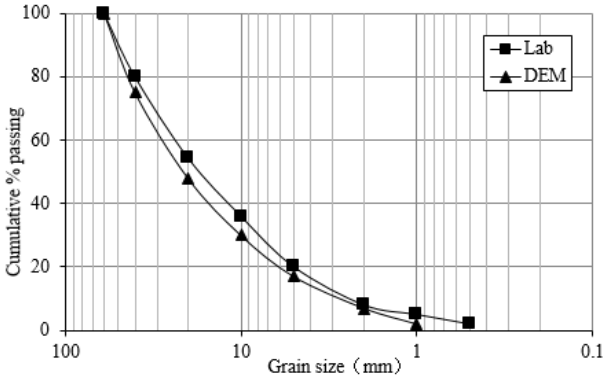

Figure 1. A comparison of the particle size distribution of coarse grained soil determined using the DEM simulation and laboratory tests.

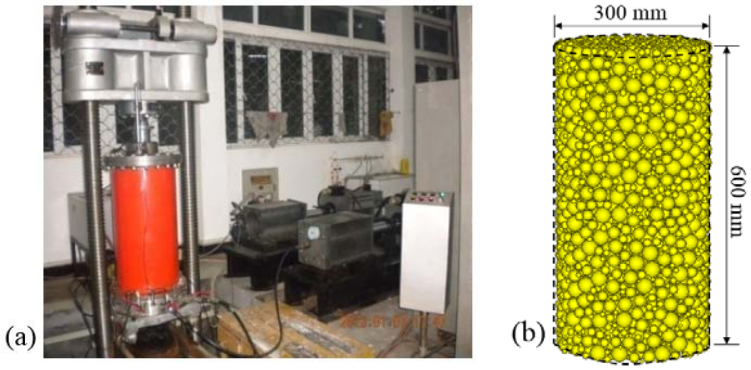

Figure 2. (a) Triaxial test in laboratory; (b) numerical model of triaxial test.

3.2. Measurement Model

A technique had been developed to determine the spatial shear surface during shearing by measuring several specific variables in a specified area. The measurement sphere is a built-in tool in PFC3D to help the user measure quantities such as coordination number, porosity, and strain rate in a specific measurement volume at the current state[12]. The diameter of the measurement sphere should be large enough and it should include at least 20 particles in calculating the average values [13].

133 measurement spheres with the diameter of 60 mm are inserted in the numerical model to calibrate the spatial shear surface. The measurement spheres are separated into 7 layers with 19 ones in each layer which are shown in Fig. 3. The spatial shear surface are determined by measuring the variation of porosity, coordination number and volumetric strain of each measurement sphere during shearing.

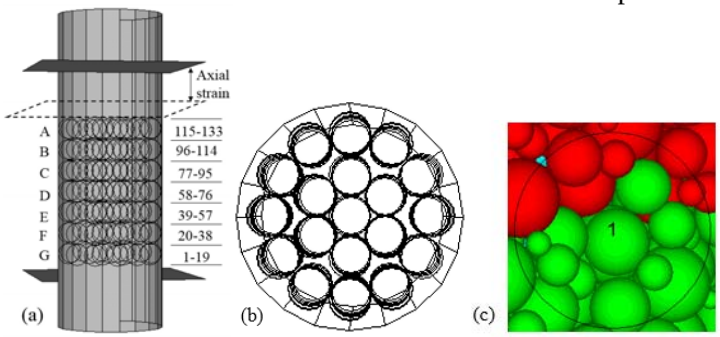

Figure 3. Distribution of measurement spheres, (a) in vertical; (b) in horizontal; (c) particles in one measurement sphere.

4. Numerical Results and Discussion

4.1. Comparison of Numerical and Experimental Results of Triaxial Test

Based on the curves of particle size distribution in numerical and experimental tests, the weighted average assembling method could keep a significant association with the experimental results after adjusting several parameters, such as the Young's modulus, inter-particle friction angle and the ratio of the normal stiffness to shear stiffness. In general, the value of Young's modulus increases as the confining stress increasing. The inter-particle friction angle is different from bulk friction angle of the granular assembly because frictional resistance is generated between particle contacts. The ratio of the normal stiffness to shear stiffness is associated with the Poisson's ratio.

The Young's modulus calibration is focus on initial slope of the shear stress-axial strain curve. The particle friction coefficient calibration is focus on the peak and residual shear strength. The comparsion of the numerical and experimental results is shown in Fig. 4. As depicted in Fig. 4, the numerical results are consistent with the laboratory results.

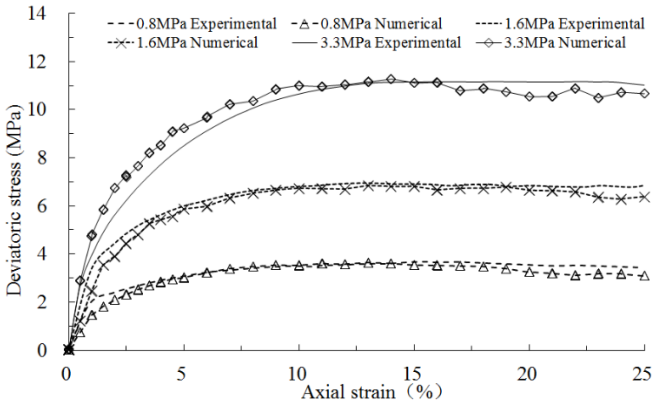

Figure 4. Comparison of the numerical and experiment results of triaxial tests.

As shown in Fig. 4, the model is in the elastic stage when the axial strain is less than 0.05. With the increase of the axial strain, cracks occur in the inter-sample between the assembled particles which leads to the plasticity of the sample. When the axial strain is 0.05-0.1, the model is in the elastic-plastic stage. As the axial strain increasing continuely, the deviatoric stress has little change that the spatial shear surface is formed and only friction resistance makes the contribution to the shear stress. At this stage, the sample is in the plastic stage and static state.

4.2. Variations of the Porosity, Coordination Number and Volumetric Strain

Spatical shear surface is formed through cracks between particles with specific characteristics of the variations of the porosity, coordination number and volumetric strain. When the contact bond is broken between two entities, the crack occurs with the movement of particles. The localized strain of the sheared area will be dilated. Therefore, the specific characteristics, such as the increase of porosity, the decrease of coordination number and the increase of the volumetric strain, are analyzed. The variations of these three parameters have been measured in each layer during shearing under the confining stress of 0.8 MPa.

Table 2. Variation of coordination number of measurement spheres of 115-123 in layer A.

Axial strain (%)	115	116	117	118	119	120	121	122	123
0	6.25	5.00	6.25	6.55	5.69	7.00	6.25	7.00	6.56
15	4.31	6.90	2.50	4.36	5.55	5.38	5.44	5.71	5.54
25	5.44	5.79	3.35	4.83	3.20	4.00	6.17	5.00	4.00
Variation (%)	-13	15.7	-46.4	-26.2	-43.8	-42.9	-1.3	-28.6	-39.1

Table 3. Variation of coordination number of measurement spheres of 124-133 in layer A.

Axial strain (%)	124	125	126	127	128	129	130	131	132	133
0	6.30	6.07	6.57	6.75	6.86	5.27	6.67	6.20	6.12	5.00
15	6.62	5.67	6.64	5.58	5.64	5.21	5.09	5.46	5.38	4.55
25	5.33	4.79	4.47	4.77	4.46	4.00	5.38	6.36	5.80	5.88
Variation (%)	-15.3	-21.1	-32	-29.4	-34.9	-24.1	-19.2	2.6	-5.2	17.5

As shown in Table 2 and 3, the variation (%) is the ratio of the value difference between axial strain of 25% and 0% to 0%. The coordination numbers in the measurement spheres of 116, 131 and 133 increase with the axial strain increase. The others decrease with different degree that the number of 117, 119 and 120 are determined as the localization of shear surface when the decrease is larger than 40%.

Table 4. Variation of porosity of measurement spheres of 115-123 in layer A.

Axial strain (%)	115	116	117	118	119	120	121	122	123
0	0.31	0.33	0.29	0.28	0.31	0.27	0.34	0.29	0.33
15	0.38	0.39	0.45	0.46	0.42	0.47	0.39	0.39	0.30
25	0.39	0.35	0.48	0.43	0.41	0.48	0.40	0.38	0.36
Variation (%)	24.32	4.96	66.59	53.43	34.74	78.60	18.99	32.90	9.99

Table 5. Variation of porosity of measurement spheres of 124-133 in layer A.

Axial strain (%)	124	125	126	127	128	129	130	131	132	133
0	0.32	0.32	0.30	0.31	0.30	0.31	0.30	0.31	0.29	0.32
15	0.38	0.37	0.34	0.37	0.45	0.34	0.41	0.37	0.33	0.41
25	0.41	0.36	0.37	0.38	0.43	0.42	0.39	0.35	0.31	0.35
Variation (%)	31.46	13.74	23.31	22.70	44.10	34.79	28.73	11.04	8.00	8.82

As shown in Table 4 and 5, porosities of all measurement spheres in layer A increase when comparing the values of porosity at the end of the shearing and the initial state. Several measurement spheres of 117, 118 and 120 are determined based on the varation of coordination number and porosity for calibrating the localization of shear surface when the increase is larger than 50%.

Table 6. Variation of volumetric strain of measurement spheres of 115-123 in layer A.

Axial strain (%)	115	116	117	118	119	120	121	122	123
0	0.00	0.00	0.00	0.00	0.00	0.00	0.00	0.00	0.00
15	0.15	0.20	0.04	0.22	0.02	0.21	0.04	-0.03	0.03
25	0.17	0.11	-0.01	0.77	0.11	0.39	0.03	-0.06	0.02

Table 7. Variation of volumetric strain of measurement spheres of 124-133 in layer A.

Axial strain (%)	124	125	126	127	128	129	130	131	132	133
0	0.00	0.00	0.00	0.00	0.00	0.00	0.00	0.00	0.00	0.00
15	0.10	-0.01	0.15	0.13	0.28	0.11	0.22	0.13	0.16	0.09
25	0.10	0.15	0.22	0.20	0.49	0.03	0.11	0.16	0.15	0.04

The volumetric strain can be calculated by measuring the volumetric strain rate in a measurement circle [13]. The variation of the volumetric strain determines the contraction or dilation behavior of the material. Shear contraction is defined as decrease in volumetric strain and shear dilation means increase in volumetric strain. When the crack occurs between particles, the volumetric strain will increase. Therefore, several measurement spheres of 120, 126, 127 and 128 as shown in Table 6 and 7 are determined to calibrate the localization of shear surface when the increase is larger than 0.2.

As mentioned above, the shear surface occurs with specific characteristics, such as the increase of porosity, the decrease of coordination number and the increase of the volumetric strain. Therfore, the determined measurement spheres in layer A for calibrating the shear surface are 117, 118, 119, 120 and 128.

Following the above method, the measurement spheres with these specific charateristics in each layers are determined, as shown in Table 8.

Table 8. The determined measurement spheres in each layer.

Layer	A	B	C	D	E	F	G
Measurement sphere	117, 118, 119, 120, 128	98, 102, 104, 109, 110	80, 83, 86, 91, 92	60, 63, 66, 69, 70, 75	40, 44, 49, 50	20, 23, 27, 29, 38	3, 5, 8

4.3. Calibration of the Spatial Shear Surface

The determined measurement spheres as shown in Table 8 are illustrated in Fig. 5 in the numerical sample. As shown in Fig. 5, the spatial shear surface is not a simple oblique plane, however, it runs through from the edge of the top plane to another lateral side and bifurcates in the internal sample.

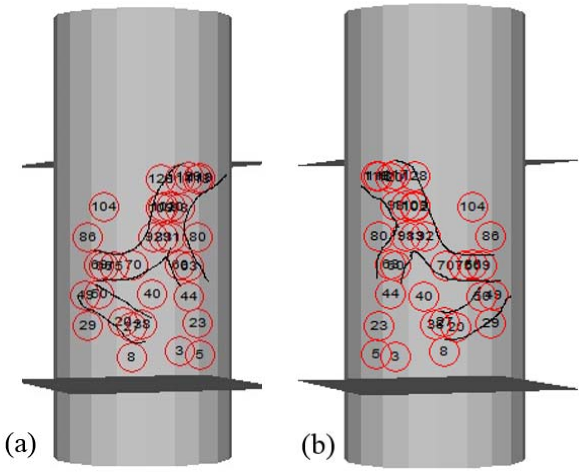

Figure 5. The distribution of spatial shear surface, (a) front view; (b) rear view.

For better understanding the suitable of the calibration of spatial shear surface using the measurement model, the rotated particle distribution are conducted. As the shear surface forming, the particles near the surface will rotated due to the relative movement [10]. The rotational velocity of particles is measured during shearing, particles are marked black color when the rotational velocity is larger than 110 rad/s. Referring to the literature of Xu [11], the theoretically spatial shear surface has been shown in Fig. 6.

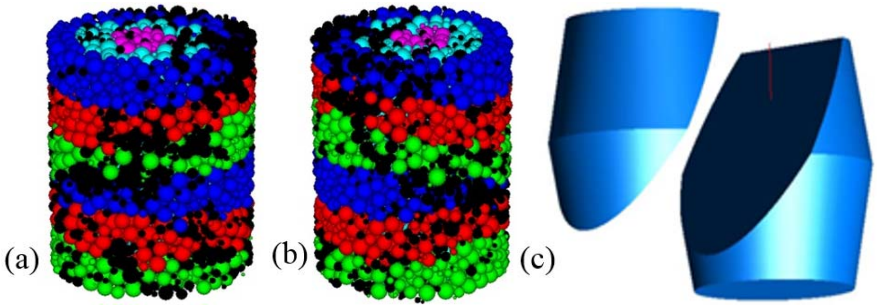

Figure 6. Spatial shear surface, rotated particle distribution in (a) front view; (b) rear view; (c) the theoretical view [11].

Comparison of Fig. 5 and Fig. 6 has been made that the spatial shear surface calibrated by the proposed measurement model is greatly consistent with that of the rotated particle distribution and the theoretical view [11]. The rotated particle distribution and the measurement model have their advantages in evaluating the distribution of spatial shear surface which is difficult to be calibrated only by the superficial cracks.

5. Conclusion

Numeircal simulations of triaxial tests are conducted with the weighted average assembling method to calibrate the spatial shear surface. Measurement model with several measurement spheres is proposed

in the model to measure the specific parameters, such as porosity, coordination number and volumetric strain. After comparing the results of the spatial shear surfaces calibrated by the measurement model, rotated particle distribution and the theoretical method, several conclusions could be made:

(1) The curve of particle size distribution made by weighted average assembling method is consistent with that of the experimental result. The numerical result of shear stress-axial strain curves has great agreement with the experimental result.

(2) The spatial shear surface is determined by locating the measurement spheres which have the charateristics of the decrease of coordination number, the increase of porosity and volumetric strain. Great consistency has been obtained in spatical shear surfaces calibrated by the measurement model, rotated particle distribution and the theoretical method.

Acknowledgments
This work was financially supported by the National Natural Science Foundation of China (51408450) and the Fundamental Research Funds for the Central Universities (2017-YB-014).

References

[1] P.A. Cundall, A computer model for simulating progressive large scale movements in blocky rock system, Proceedings of the Symposium of the International Society of Rock Mechanics (Nancy, France), Vol. 1, Paper No. II-8, 1971.
[2] V.B. Stefan, Discrete element analysis of granular materials, Nederland: Proefschrift Technische Universiteit Delft, 1996.
[3] H.B. Muhlhaus, I. Vardoulakis, The thickness of shear bands in granular materials, Geotechnique 37(1987) 271-283.
[4] M. Oda, K. Iwashita, Study on couple stress and shear band development in granular media based on numerical simulation analyses, Int. J. Eng. Sci. 38 (2000) 1713-1740.
[5] Z.H. Zhang, G.D. Zhang, X.L. Li, Z.H. Xu, The Shear Dilation and Shear Band of Coarse Grained Soil Based on Discrete Element Method, Appl. Mech. Mater. 744-746 (2015) 679-685.
[6] M.J. Jiang, X.M. Li, Y.G. Sun, H.J. Hu, Discrete element simulation of biaxial compression test considering rolling resistance, Rock Soil Mech. 30 (2009) 514-517.
[7] M. J. Jiang, F.Z. Wang, H.H. Zhu, Shear band formation in ideal dense sand in direct shear test by discrete element analysis，Rock Soil Mech. 31 (2010) 253-257.
[8] I.G. Vardoulakis, B. Graf, Imperfection sensitivity of the biaxial test on dry sand. IUTAM: Conference on Deformation and Failure of Granular Materials, Deft: 485-491 (1982)
[9] J. Zhou. Micro model tests and numerical simulations of geomechanics, Beijing: Science Press, 45-72 (2008)
[10] Z.H. Zhang, X.D. Zhang, H.S. Qiu, L. Wu, Y.S. Deng, Weighted average assembling method using in triaxial numerical experiment based on PFC3D, J. Wuhan Uni. Tech. (Transport. Sci. Eng.) 41(2017) 263-267.
[11] Z. H. Xu, Study on state dependent constitutive model incorporating particle breakage for coarse granular material, Yichang: China Three Gorges University (2014)
[12] Itasca Consulting Group Inc., a state (the Universal Distinct Element Code), Version 4.0. Minneapolis: ICG (2004)
[13] Y. Cui, A. Nouri, D. Chan, E. Rahmati, A new approach to DEM simulation of sand production, J. Petrol. Sci. Eng. 147(2016) 56-67.